CHARACTERIZATION OF THE DAMAGE MECHANISMS IN POLYMER COMPOSITE MATERIALS BY ULTRASONIC WAVES, ACOUSTIC EMISSION AND INFRARED THERMOGRAPHY

W Harizi, S Chaki, G Bourse, Mohamed Ourak

CHARACTERIZATION OF THE DAMAGE MECHANISMS IN POLYMER COMPOSITE MATERIALS BY ULTRASONIC WAVES, ACOUSTIC EMISSION AND INFRARED THERMOGRAPHY

W. Harizi[1*], S. Chaki[1], G. Bourse[1], M. Ourak[2]

[1]*Département Technologie des Polymères et Composites et Ingénierie Mécanique, Ecole des Mines de Douai, 941 rue Charles Bourseul BP 10838, 59508 Douai Cedex, France*

[2]*Département d'Opto-Acousto-Electronique, IEMN, URM CNRS 8520, Université de Valenciennes, Mont Houy BP 311, 59313 Valenciennes, Cedex, France*

*walid.harizi@mines-douai.fr

Keywords: Polymer Composite Materials (PCM); Ultrasonic waves; Acoustic Emission; Infrared thermography

Abstract

In this study, Non-Destructive Testing (NDT) of the Polymer Composite Materials damage mechanisms by combining three techniques, namely ultrasonic waves, acoustic emission and infrared thermography was achieved. Longitudinal waves in C-scan representation were used to characterize initial state of the tested materials, where high resolution maps of velocity, attenuation and density were obtained and analyzed. The Acoustic Emission (AE), InfraRed (IR) thermography and Lamb waves techniques were used for detection and identification of the occurred damage mechanisms under mechanical loading. The principal result of this work is the development of an experimental technique for NDT combined tests to assess the damage according several different signatures.

1. Introduction and objectives

Different types of PCM have recently been introduced and studied in different scales from macro to nano composites **[1]**. Cross-ply Glass Fiber Reinforced Polymer (GFRP) laminates are strongly used in various fields because they are lightweight materials, resistant to corrosive environments and exhibiting remarkable mechanical and physical properties. The implementation of this type of material has several phases; the more critical is the crosslinking of the epoxy matrix. During this stage, plate changed from stacking of prepreg plies to the state of rigid structure in which the polymerization is accompanied inevitably by the appearance of defects in form of closed porosities whose shape, size and distribution are highly variable depending on the material and manufacturing process **[2]**. Several mechanisms of damage may appear from these manufacturing defects due to mechanical loading. They are generally: the matrix cracking, the interfacial debonding between the fiber and matrix or the

pull-out, fiber breakage and the delamination between plies for laminated composites **[3-4]**. It is very important to dispose of some methods able to detect not only the manufacturing defects in the initial state (before loading), but also to follow the damage evolution in the sample under or after mechanical loading. The ultrasonic method in C-scan mode can be used to visualize defects and characterize the mechanical properties of materials through measurements of velocity and attenuation. They are two parameters sensitive to damage, and cannot be measured without knowledge of the local thickness of the studied sample. In the reference **[5]**, *Graciet and Hosten* describe a hybrid method for simultaneous determination of these four parameters. The Lamb waves also have significant interest in NDT of PCM because they can propagate across a long distance. However, they are dispersive and multimodal, thus more difficult for use and interpretation than the conventional ultrasonic method. They were used to detect the damage when the Lamb wave velocity decreased **[6]**.

Under mechanical loading, the AE technique is widely used for detection and real-time monitoring of PCM damage. The amplitude of the AE signals is by far the most used discriminator of acoustic signatures **[4]**.

The IR thermography is a promising NDT technique for characterization of composite materials. This technique provides easily and quickly the surface defect mapping of the samples and can also detect a relatively deep defects in lock-in mode. Quite rarely the last three techniques were used simultaneously for characterizing the integrity of composite materials, except the work of Kim and Liaw **[7]**.

This study deals with characterization of the GFRP damage under mechanical loading by combining three NDT techniques: ultrasonic waves, AE and IR thermography. The initial state of the specimens is characterized by C-scan, where maps of velocity, attenuation and density obtained with high resolution allow detection of weakness areas and may predict the final fracture location. The mechanical loading is a monotonic tensile test performed in progressive steps. The real time monitoring of the damage is carried out by two AE resonant sensors during each load phase. In the bearing steps (when stress is constant vs. time), the acquisition of AE is temporarily stopped and one of the two sensors is excited to generate the first symmetric $\mathbf{S_0}$ mode and the second sensor is in reception mode. The $\mathbf{S_0}$ mode is linked with the Young's modulus of the material; its evolution during different loading levels gives the stiffness of the test specimen, so we can evaluate its damage. The IR thermography is in continuous acquisition during all loading phases. The combination of these three techniques is performed to evaluate the PCM damage under mechanical loading with three different signatures, which will increase the reliability of the characterization.

2. Theoretical approaches

2.1. C-scan test

The experimental device (fig.1.a) used in this study consists of two stainless steel plates rectified with parallel planes and deposited on two Plexiglas glued to the bottom of the water tank. The PCM specimen, deposited on these two gauge blocks of stainless steel, has the following properties: thickness e, density ρ_1, longitudinal wave velocity V_1 and attenuation coefficient α. This sample is totally immersed in water. A focused transducer in normal incidence works in pulse echo mode. The initial pulse launched by the transducer, $S_0(t)$, propagates through the coupling fluid and reflected on the water/sample interface to produce the echo $S_2(t)$. The part of the pulse, echo $S_3(t)$, transmitted through the sample is reflected at the second interface sample/water from the back surface of the specimen. The echo $S_1(t)$ is the reference pulse that is reflected at the interface between water and a stainless steel plate. Here a perfectly flat surface of stainless steel was chosen because the reflection coefficient is close to unity and well known ($R_{03}=0.936$ with $\theta_{water} = 20°C$). An A-scan representation of S_1 and (S_2, S_3) signals is shown in fig.1.b. Let t_1, t_2 and t_3, the time of light of echoes S_1, S_2 and S_3, respectively. So, it is possible to determine the thickness of the sample e by $e = \frac{V_0}{2}(t_1 - t_2)$ and the longitudinal wave velocity V_1 by $V_1 = V_0 \frac{(t_1 - t_2)}{(t_3 - t_2)}$ where $V_0 = 1480\ m/s$ is the water velocity at 20°C.

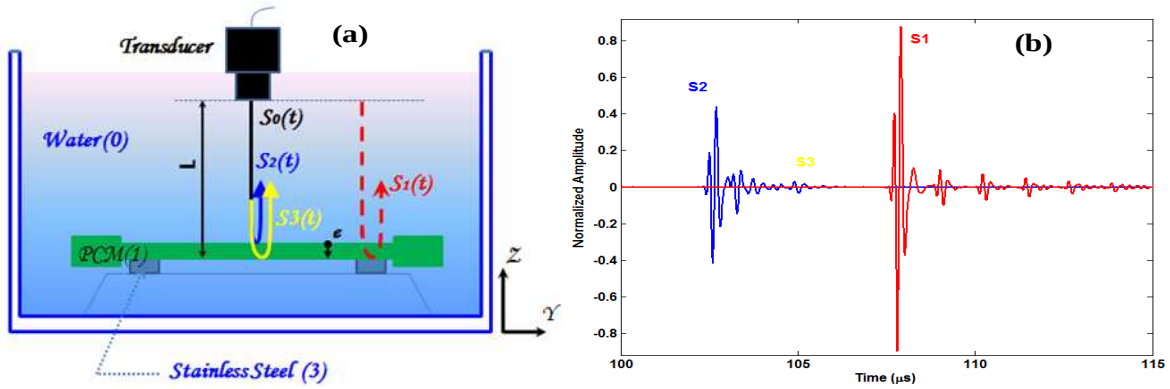

Figure 1. (a) Experimental device of C-scan test, (b) temporal representation of $S_1(t)$ and ($S_2(t)$, $S_3(t)$) signals

If we use $A_i(f)e^{-j\theta_i(f)}$ to represent the Fourier transform of a pulse $S_i(t)$, the Fourier transforms of the three signals can be expressed as:

$$S_1(f) = A_1(f)e^{-j\theta_1(f)} = S_0(f)e^{-2(\alpha_0+j\beta_0)L}R_{03} \quad (1)$$

$$S_2(f) = A_2(f)e^{-j\theta_2(f)} = S_0(f)e^{-2(\alpha_0+j\beta_0)(L-e)}R_{01} \quad (2)$$

$$S_3(f) = A_3(f)e^{-j\theta_3(f)} = S_0(f)e^{-2(\alpha_0+j\beta_0)(L-e)}e^{-2(\alpha+j\beta)e}(-R_{01})T_{01}T_{10} \quad (3)$$

where $S_0(f)$, $S_1(f)$, $S_2(f)$, $S_3(f)$ are the Fourier transforms of $S_0(t)$, $S_1(t)$, $S_2(t)$ et $S_3(t)$ respectively. α_0 and α are the attenuation coefficients, and β_0 and β are the propagation constants, of the water and the specimen, respectively. L is the distance between the transducer and the steel stainless plates as shown in fig.1.a. R_{01} is the reflection coefficient at the water-specimen interface, T_{01} is the transmission coefficient at water-specimen interface but T_{10} is the transmission coefficient at the specimen-water interface. We put $T = T_{01}T_{10} = 4Z_1Z_0/(Z_1+Z_0)^2$ the overall transmission coefficient when the pulse passes through the interface twice where $Z_1 = \rho_1 V_1$ and $Z_0 = \rho_0 V_0 = 1{,}48.10^6 kg.m^{-2}.s^{-1}$ at 20°C. We now consider sample thickness and longitudinal wave velocity determined from the signal shown in fig.1.b. With the same acquired signals, we are interested in the determination of the two other quantities: material density and wave attenuation. Then, we define the amplitude $B_i(f_0)$ of the echo *i* relatively to the reference signal S_1 by: $B_i(f_0) = \frac{|S_i^*(f_0)|}{|S_1^*(f_0)|}$ at frequency f_0. B_2 represents the ratios of two reflection coefficients and does not depend on frequency. One can obtain the density ρ_1 and the attenuation α (eqs.4) by combining equations (1), (2) and (3) with the expression of $B_i(f_0)$. Attenuation and density can be reached from the determination of the Fourier transforms modulus of the two first echoes.

$$\rho_1 = \frac{Z_0}{V_1}\left(\frac{1+B_2|R_{03}|}{1-B_2|R_{03}|}\right) \qquad \alpha(f_0) = -\frac{1}{2e}\ln\left(\frac{B_3(f_0)|R_{03}|}{|R_{01}|T}\right) \quad (4)$$

2.2. Bulk wave and damage ultrasonic variable

The knowledge of the elastic constants C_{ij} of a material allows calculating the velocities V_{ij} for any propagation direction. In the evaluation of heterogeneous materials, one must solve the inverse problem which deals with the determination of elastic constants from measurements of ultrasonic propagation velocities. In the principal directions, simple relationships can be established between the diagonal elastic constants and the propagation velocities **[8]**. The quasi transverse isotropic materials (tetragonal system) are invariant under 90° rotation about the Z axis (axis 3). In this case, the axis 1 and 2 (fig.2.a) are equivalent.

Consider the Christoffel equation $\Gamma_{il} - \rho V^2 \delta_{il}$ (where Γ_{il} is the Christoffel tensor and δ_{ij} is the Kronecker symbol which equals 1 if i=j and 0 if i≠j) for a wave moving in the principal directions for a quasi transverse isotropic material, the propagation tensor takes a simple form in each direction **[8]**. The expressions of velocities as a function of elastic constants are the following:

$$\begin{cases} \rho V_{11}^2 = \rho V_{22}^2 = C_{11} \\ \rho V_{33}^2 = C_{33} \\ \rho V_{13}^2 = \rho V_{23}^2 = C_{44} \\ \rho V_{12}^2 = C_{66} \end{cases} \quad (5)$$

If we determine the stiffness constants by ultrasonic measurements, we can evaluate the damage factor ***D*** of the material along the principal directions by using eq.(6) where C_{ij}^0 is the stiffness constant of the material in the initial state.

$$D_{ij} = 1 - \frac{C_{ij}}{C_{ij}^0}; i = j \quad (6)$$

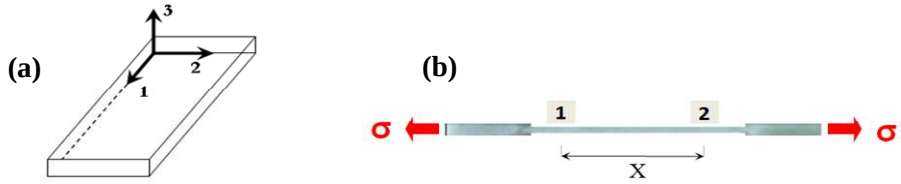

Figure 2. (a) Principal axis of composite material and (b) measurement of Lamb waves

2.3. Lamb wave velocity

The distance between transducers (1) and (2) (fig.2.b) increases with the strain after application of a stress σ. If we denote by X the distance between the centers of the two transducers at zero strain, the wave velocity at strain ε can be calculated as $V(\varepsilon) = \frac{X(1+\varepsilon)}{t_R}$ where t_R is the arrival time at the receiver for this strain. The wave velocity in the principal axis of the orthotropic laminate for low frequency-thickness product values is expressed by $V = \sqrt{\frac{A_{11}}{\rho e}} = \sqrt{\frac{E_1}{\rho(1-v_{12}v_{21})}}$ where A_{11} is the longitudinal in-plane stiffness for the entire plate, E_1 is the longitudinal Young's modulus, and v_{12} and v_{21} are the major and minor Poisson's ratios **[6]**. For the GFRP laminates investigated in this study, $1 - v_{12}v_{21} \approx 1$ and hence we can obtain the eq.(7).

$$E_1 = \rho V^2 \quad (7)$$

3. Experimental procedures

3.1. Material subject of study

The test material was cross-ply GFRP laminates with lay-ups of $[0°/90°]_S$. It was made from unidirectional sheets of E type glass fibers pre-impregnated with uncured epoxy. E-glass balanced fabric is used to incorporate heels to the plates in order to have specimens for mechanical tests. The manufacturing process of the PCM plates used in this study was optimized to obtain, as far as possible, coplanar plates with uniform thickness; this requirement will gives good conditions for ultrasonic measurements. To achieve this requirement, we opted for compression molding and the heels were built through twill tape 2/2, whose fibers are oriented at 45°, integrated on both ends of the stack according to NF EN ISO 527-5. The tensile specimens are cut from the plates by using diamond-wheel saw, their dimensions are shown in figure 3 and detailed in table 1. Given the heterogeneity of composite materials, all samples tested in this study belong to the same PCM plate.

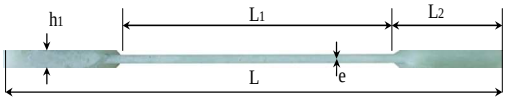

Figure 3. The sample mechanical test

Symbols	Designation	Values (mm)
L	Total length	250
L_1	Distance between heels	150±1
L_2	Length of heels	≥ 50
b	Width	20±0,5
e	Thickness of the specimen	3,5 ±0,2
h_1	Thickness of the heels	7,5

Table 1. Dimensions of specimens

It should be noted that $[0°/90°]_S$ configuration corresponds to a quasi transverse isotropic material.

3.2. Test procedures

Before the loading test, three PCM samples are scanned to characterize their initial state after the manufacturing process as shown in fig.1.a. A 5 MHz focused transducer (NDT-Automation) with a diameter of 12.7 mm and a focal distance of 63.5 mm was used in normal incidence. The figure 4.a illustrates the experimental setup and the mechanical loading profile (fig.4.b) used in this study. The PCM specimen is equipped with three transducers, the transducers 1 and 2 are both piezoelectric resonant (300 kHz), type Nano 30 (Physical Acoustics Corporation (PAC)) with a bandwidth of 125-750 kHz, ϕ = 8 mm. The transducer 3 (Panametrics M109, ϕ = 12.7 mm) which generates longitudinal waves at 5 MHz is located on the other face of the specimen. The mechanical loading is driven by an electric tensile machine with a capacity of 100 KN at a deformation rate of 0.5 mm/min. For all loading steps, AE activity will be detected by both sensors 1 and 2, amplification is made by two preamplifiers (PAC, 20-1200 kHz, 40 dB). The AE signals are recorded to the AE device for digital acquisition and signal processing. At each step corresponding to a constant loading, the acquisition of AE events (between yellow dashes) is stopped and the two AE sensors will be used to generate and receive Lamb waves: the US computer emits a tone burst of 5 cycles at a frequency of 200 kHz, duration of 25 μs and with a voltage of ±40 V. The high voltage (HV) tone burst excites the transducer 1 as an emitter. The transducer 2, at a distance of X=120 mm from the first, receives the Lamb wave consecutively, acquired and registered to oscilloscope (LeCroy wave Runner 44Xi, 5GS/s) at channel 1. The experimental setup for the Lamb wave generation and detection during a loading test is plotted (blues dashes) in fig.4.a. The pulse generator (Panametrics 5077PR) excites the transducer (3) by square pulse of 400 V with a gain of 10 dB. The longitudinal wave made a round trip in the thickness of the specimen and will be recorded on the oscilloscope. The excitation circuit with the longitudinal wave is represented with interrupted orange dashes. The generation and the excitation with the Lamb and longitudinal waves are favored to the beginning of each step while loading is constant, at least 1.5 minutes. IR thermography is in continuous acquisition during loading and maintaining steps. After 1.5 minutes in each maintaining step, we excite two halogen lamps (P=1000 W) with three sine cycles at 0.1 Hz. The handling is done without contact with the external environment to limit its influence and avoid all problems that can damage the thermographic measurement, which was made by the use of the black blankets covering the mechanical tensile machine and all the equipments already described before.

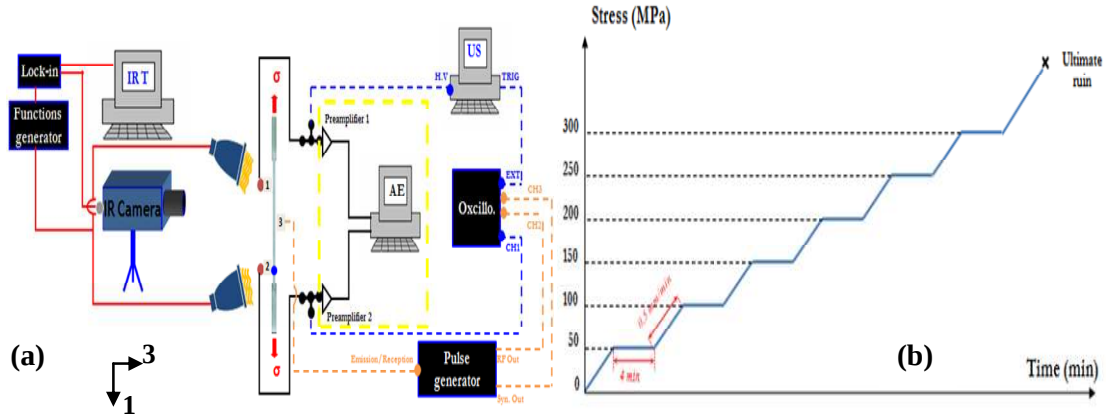

Figure 4. (a) The experimental setup and (b) the mechanical loading profile for the combined tests

4. Results and discussions

4.1. Ultrasonic C-Scan

The figure 5 presents the C-scan results of one specimen from the three others. We are interested specifically in velocity (1st column), density (2nd column) and attenuation (3rd column) maps. It is clear that high velocities obtained for PCM induce high densities, this quantity is between 1000 (pure resin) and 2500 Kg/m^3 (fibers concentrations). Significant attenuation values are distributed along lines perpendicular to the length of the specimens, this explains how the 90° plies attenuate the longitudinal waves in thickness samples. We can clearly see that all maps are heterogeneous, this specificity corresponds to PCM samples.

4.2. AE method

Loading results are shown in fig.6 with the acoustic activity in terms of the AE signals amplitude (fig.6.a) and their percentage (fig.6.b). Ninety percent of the acoustic activity is recorded during the last two stages of mechanical loading. To discriminate clearly the different damage mechanisms, it is advantageous to use a multivariate statistical analysis that will be the subject of subsequent study.

4.3. Ultrasonic velocities propagation

The figure 7.a shows the longitudinal wave velocity V_{33} recorded before and during all steps at constant loading. It decreases considerably just at the final level. We calculate the damage factor $\boldsymbol{D_{33}}$ (fig.7.b) from the equation (6) in this direction. The $\boldsymbol{D_{33}}$ value is near zero for the first five steps then it increases at the last stage; that allows concluding that we cannot detect damage in the direction (3) with this method. Typical forms of Lamb waves signals are represented in fig.8.a for the initial state and for the 6 levels of constant loading. We may observe a high decrease of the signal amplitude with the increase of the stress level between 100 and 300 MPa. We also observe changes in the shape of the signal, which implies changes in spectral content of the signals. The damage factor $\boldsymbol{D_{S0}}$ (fig.8.b), is equal to zero up to 50 MPa and then increases until high values showing the increase of damage in the sample. $\boldsymbol{D_{S0}}$ is more significant than the $\boldsymbol{D_{33}}$, so the $\mathbf{S_0}$ mode is able to characterize the state of damage of PCM.

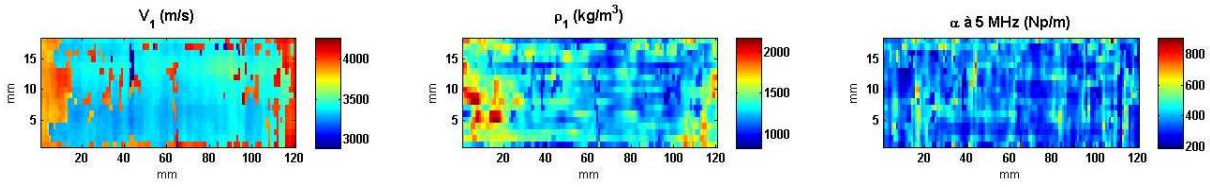

Figure 5. C-scan results

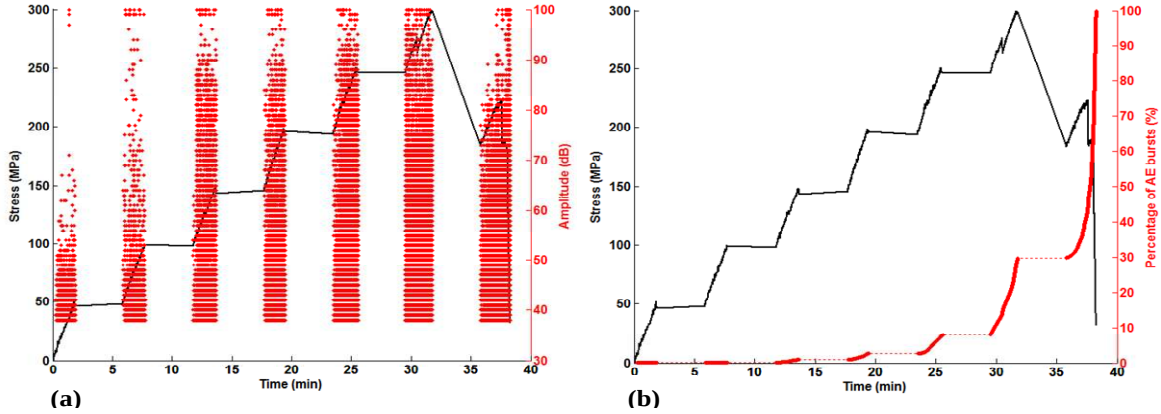

Figure 6. (a) Amplitude and (b) percentage of AE activity in combined tests

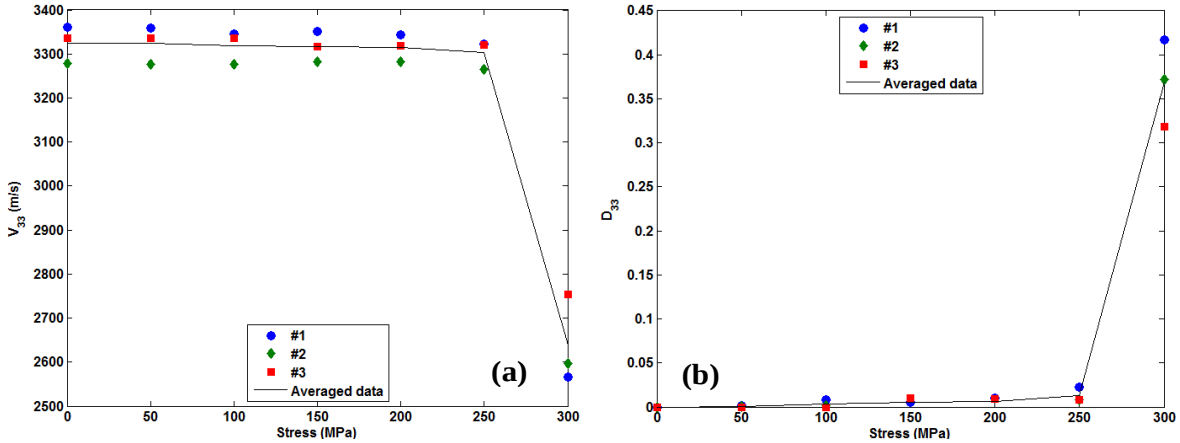

Figure 7. (a) Longitudinal wave velocity V_{33} and (b) the damage $\boldsymbol{D_{33}}$ vs. stress

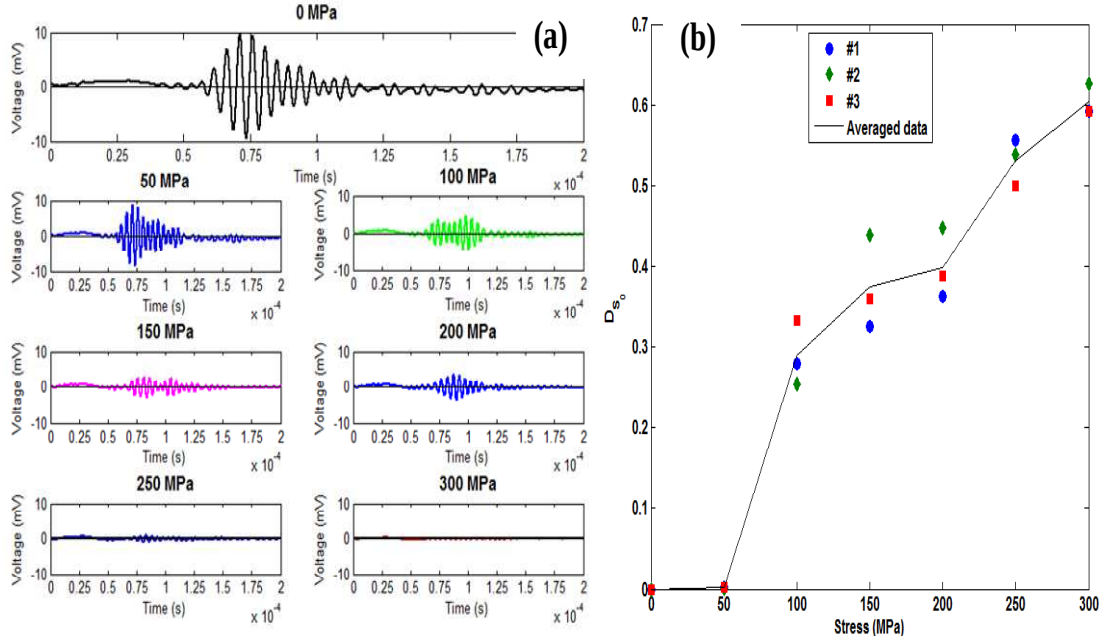

Figure 8. Typical forms of Lamb waves (a)Young's modulus and (b) the damage $\boldsymbol{D_{S0}}$ vs. stress

4.4. IR thermography

The evolution of the average temperature as function of time is shown in fig.9.a for an interest zone (90 mm of the total length X entire width). In each level of constant loading, the specimen is excited with the halogen lamps which explain the temperature peaks. These combined tests are not easy to realize because they are manually made, that may explain the experimental defect at level warming n°5 where the sample was excited with a sine signal with only two cycles. IR thermography during these combined tests has shown its reliability to detect matrix cracks that develop at 0° plies of PCM (fig.9.b and c).

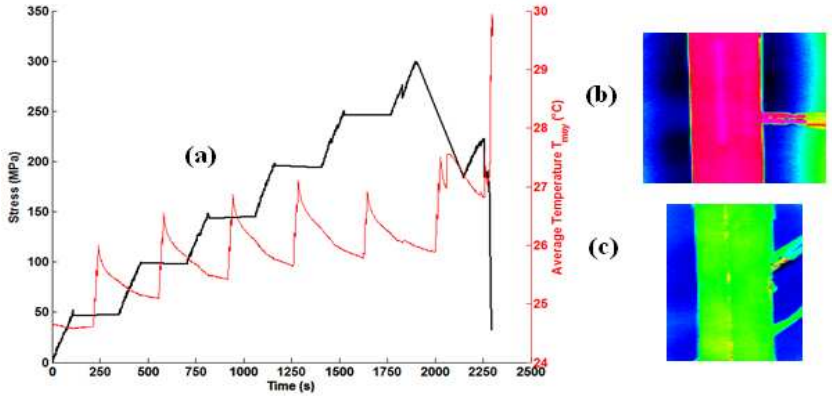

Figure 9. (a) Profile of the temperature in the differents steps of the mechanical loading and longitudinal craks in (b) #1 and (c) #2

5. Conclusions

This study has shown that a combination of three NDT can be realized under a monotonic loading testing. It was thus possible to assess the damage of PCM according these different techniques. The Lamb waves have shown greater sensitivity to the damage that the longitudinal waves. The AE data treatment requires multivariate analysis to classify them according four main damage mechanisms that may appear in this type of material; this is outside of this framework for a future publication. The IR thermography has shown its reliability to detect matrix cracks.

References

[1] Colombo C., Vergani L., Burman M. Static and fatigue characterization of new basalt fibre reinforced composites. *Composite structures*, 94, pp. 1165-1174 (2012).

[2] Ledru Y., Piquet R., Michel L., Schmidt F., Berhnart G. *Quantification 2-D et 3-D de la porosité par analyse d'images dans les matériaux composites stratifiés aéronautiques* in "Proceeding of *Comptes Rendus des JNC 16*, Toulouse, France, (2009).

[3] Berthelot J.M., *Matériaux composites-Comportement mécanique et analyse des structures*. 3ème édition. Paris Editions Tech. & Doc. (1992).

[4] Barré S., Benzeggagh M.L. On the use of acoustic emission to investigate damage mechanisms in glass-fibre-reinforced polypropylene. *Composites Science and Technology*, 52, pp. 369-376 (1994).

[5] Graciet C., Hosten, B. Simultaneous measurement of speed, attenuation, thickness and density with reflected ultrasonic waves in plates, *Ultrasonics Symposium*, pp. 1219-1222 (1994).

[6] Dayal V., Kinra V. Leaky Lamb waves in an anisotropic plate.II: Nondestructive evaluation of matrix cracks in fiber-reinforced composites. *J. Acouct. Soc. Am.* 89 (4), pp. 1590-1598 (1991).

[7] Kim J., Liaw P. Monitoring tensile damage evolution in Nextel 312/Blackglass composites. *Materials science and Engineering*, A 409, pp. 302-308 (2005).

El Guerjouma R., Goujoun L., Nechad H. Linear and nonlinear ultrasonics for material damage evaluation and health monitoring. Revue Matériaux et Techniques, pp 48-50 (2002).